REVIEW OF CALCULATION ANALYZES AND TESTS OF THE SW-4 SOLO HELICOPTER IN VARIOUS CONFIGURATIONS

Jakub Solarski
„PZL-Świdnik" S.A. Leonardo Helicopters Company
Świdnik, Poland

Radosław Raczyński
„PZL-Świdnik" S.A. Leonardo Helicopters Company
Świdnik, Poland

Adam Rosłowicz
„PZL-Świdnik" S.A. Leonardo Helicopters Company
Świdnik, Poland

Wiesław Kanadys
„PZL-Świdnik" S.A. Leonardo Helicopters Company
Świdnik, Poland

Abstract

This article presents an overview of issues related to the trials of the SW-4 SOLO helicopter in various configurations resulting from HELIMARIS and RPAS In Air projects. It covers a wide range of activities carried out by Engineering and Flight Line teams, both in the areas of calculation analyses and as a result of simulation studies, flight and ground tests. The subject of the document covers findings of two projects in which the SW-4 SOLO helicopter took part. One of them is the OCEAN2020 Project, in particular the part concerning the HELIMARIS stage with helicopter modification for the needs of over water operational capabilities, and the other is the RPAS In Air Project, where the main configuration change was innovative implementation of the system for satellite communication and a series of tests demonstrating the possibility of controlling an unmanned aerial vehicle with the use of a satellite data link.

1. NOTATION[1]

Symbols

C_d	Drag coefficient, -
C_p	Pitching moment coefficient, -
C_y	Yawing moment coefficient, -
l	Reference length, m
H_p	Pressure altitude, m
S	Reference area, m^2
t_2	Double-amplitude time
T	Oscillation period
V_H	Maximum cruise speed, km/h
V_{NE}	Never-exceed Speed
φ	Roll angle, deg
ψ	Yaw angle, deg
θ	Pitch angle, deg

Acronyms:

AFCS	Automatic Flight Control System
AoA	Angle of Attack
ATM	Air Traffic Management
BRLOS	Beyond Radio Line of Sight
C2	Command and Control
CAD	Computer Aided Design
CFD	Computational Fluid Dynamics
CoG	Center of Gravity
CTO	Ship Design and Research Center
EFS	Emergency Floatation System
FCS	Flight Control System
h/c	helicopter
GCS	Ground Control Station
IAS	Indicated Airspeed
ISA	International Standard Atmosphere
IGE	In-Ground Effect
HMI	Human-Machine Interface

IMU	Inertial Measurement Unit
ISA	International Standard Atmosphere
JAR/FAR	Joint Aviation Requirements
MCP	Maximum Continuous Power
MR	Main Rotor
MTOW	Maximum Take-Off Weight
OAT	Outside Air Temperature
OGE	Out of Ground Effect
ROC	Rate Of Climb
RPAS	Remotely Piloted Aircraft System
RUAS	Rotorcraft Unmanned Aerial System
SAS	Stability Augmentation System
SL	Sea Level
TAS	True Airspeed
TET	Tetrahedral element
TOP	Turbine Outlet Power
TOT	Take-Off Temperature
TOW	Take-Off Weight
TR	Tail Rotor
UDF	User Defined Function
VBM	Virtual Blade Model
WUT	Warsaw University of Technology

2. INTRODUCTION

The SW-4 SOLO helicopter is an object containing adequate modifications of the structure enabling the performance of sea missions and cooperation with vessels in an unmanned operational variant. From the point of view of the possibility of modifying the helicopter, two configuration variants were indicated. The first representing equipment dedicated to maritime missions (Figure 1) and the second representing equipment dedicated for unmanned operations (Figure 2) where the SATCOM Datalink, operating in Ka-Band frequency, allow BRLOS bidirectional transmission of data, HD video and commands between the GCS and the SW-4 SOLO helicopter.

Both of these configurations can be used to cooperate with a vessel (Fig. 3), that possibilities of cooperation were analyzed as part of earlier modifications, the results of which were presented at the 45th ERF.

3. SW-4 SOLO MARITIME VERSION

3.1. Definition of the test object

Increasing the operational capabilities of the helicopter requires the introduction of design changes that have a significant impact on the aerodynamic and aeromechanics characteristics of the helicopter, and thus on static, directional, dynamic stability and helicopter performance. Changing the operational conditions of the helicopter (operations in the vicinity of the vessel) requires additional numerical validation confirming the capacity and confirming safety during the mission. The main areas to be modified included:

- active safety system based on the EFS floatation system, activated automatically (by indicators deployed on helicopter structure/ manually (activated by pilot) in the case of contact between the helicopter and the water surface;
- SATCOM antenna allowing the data transfer between the on-board systems and the ground control station;
- anchoring system for enabling landing of the helicopter on board of the vessel.

Figure 1: SW-4 SOLO in OCEAN2020 configuration. Credits: PZL-Świdnik.

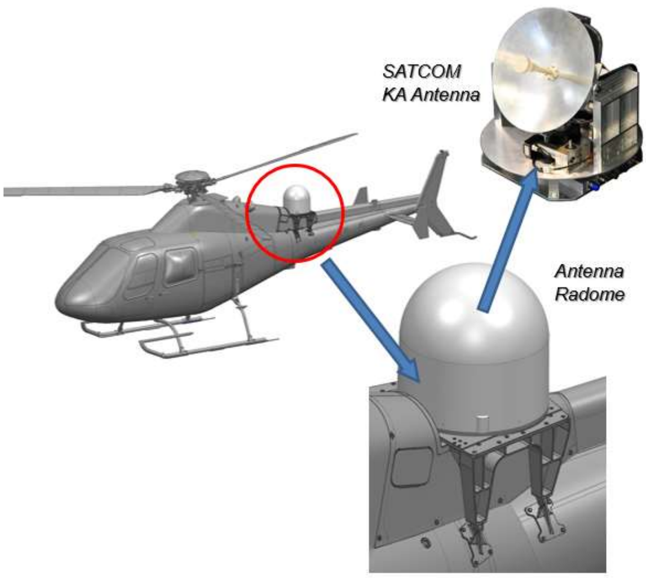

Figure 2: SW-4 SOLO in RPAS In Air configuration. Credits: PZL-Świdnik.

Figure 3: Visualization of vessel T-23 class. [7]

3.2. Adaptation oft he Helicopter structure

3.2.1. Emergency flotation system

Laboratory hydrostatic and hydrodynamic tests carried out on a scale helicopter allowed the development and validation of a numerical model whose purpose is to shorten the design iteration loop and provide the evidence required by EASA during future certification activities. The research strategy was based on a scheme for evaluating the helicopter's qualities in terms of buoyancy stability and ditching on water in the conditions of proper activation of the EFS system and in the conditions of damage to one of the float sections. The following figure shows the visualization of the helicopter 1:8 model in scale (Fig. 4 a) and the corresponding numerical twin (Fig. 4 b). The analysis related to hydrostatics also includes the problem of helicopter stability on a wave. Similarly to buoyancy analyses, the digital twins approach was used.

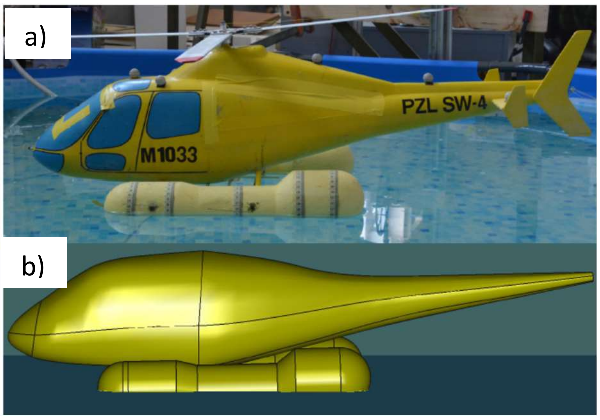

Figure 4: Visualization of the SW-4 SOLO a) scale model b) numerical model. Credits: CTO/ PZL-Świdnik

In accordance with the interpretation of the provisions of AC 27.801 and the design assumptions, object's buoyancy was tested, for sea state 5min (correct filling of EFS) and for and for sea state 2 in case of EFS system malfunction. The characteristics of the wave for which the stability values are assessed are shown in figure 5.

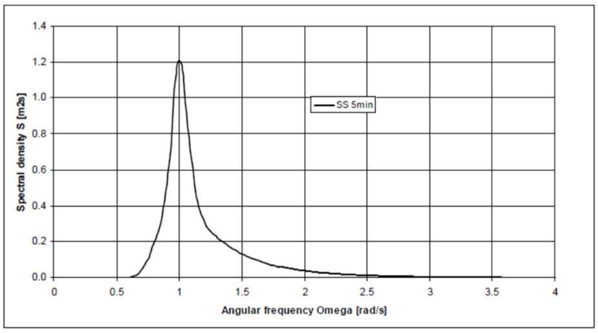

Figure 5: Wave spectrum for sea state 5 min. Credits: CTO/ PZL-Świdnik

In order to confirm the safety levels, numerical analyzes and experimental validation were performed (Fig. 6), allowing determination of hydrostatic characteristics of the object required in the process of proving compliance with EASA rules and regulations.

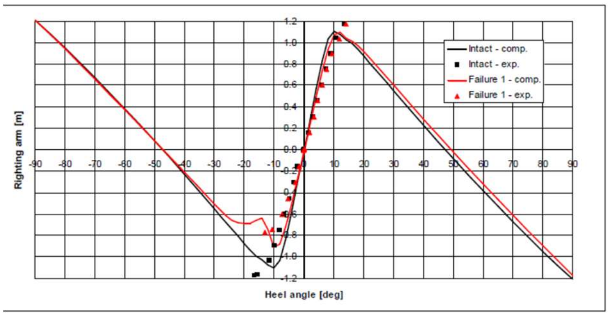

Figure 6: Static stability – righting arm. Credits: CTO/ PZL-Świdnik

The design of the helicopter that would enable its proper maritime mission performance, should ensure safety in the event of an emergency ditching. In order to determine the maximum accelerations, the helicopter model intended for laboratory tests was modified and equipped with an acceleration and pressure measurement system. The helicopter model reproduces the mass and geometric features and has a precession corresponding to the real object.

Figure 7: Sensor location a) accelerometers b) pressure. Credits: CTO/ PZL-Świdnik

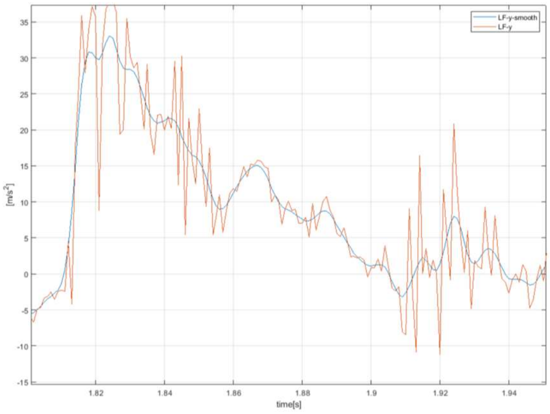

Figure 8: Time plots of accelerometers in measuring points. Credits: PZL-Świdnik

The arrangement of the sensors will allow to determine the acceleration values in the areas of the helicopter, i.e. in the h/c center of gravity and under the pilot's seat. The determined values of the maximum accelerations as well as the dynamic pressure parameters will serve as input data in the static and fatigue strength analyses.

3.2.2. SATCOM installation safe analysis

In order to ensure the safety of the mission, the unmanned helicopter is equipped with the SATCOM satellite communication system, ensuring signal transmission regardless of the geographical location of the h/c. The installation of the system requires modification of the structure, which may affect the flight performances and properties of the helicopter. Due to the relatively large sizes dimensions of the antenna (compare to overall fuselage dimension), the selection of the installation position requires consideration of many factors, such as the helicopter's balance (cg position), the influence of the antenna's fairings on aerodynamic disturbances and the resistance of the antenna structure to thermal and aerodynamics loads as a resulting from the flow of free stream and exhaust gases.

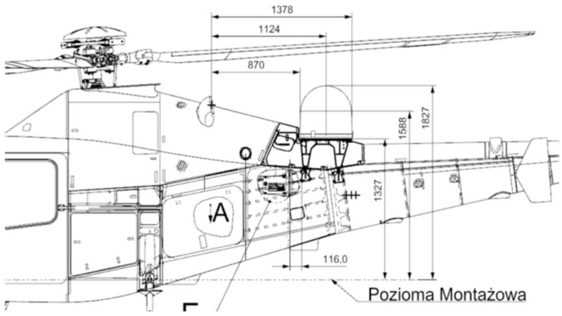

Figure 9: General view of SW-4 SOLO configuration. Credits: PZL-Świdnik

The first stage of the safety assessment assumes the determination of the aerodynamic characteristics of the fuselage with the built-in satellite antenna. Fig. 9 shows the visualization of the hull flow around in the version with the built-in antenna (Fig. 10a) and for the serial variant (Fig. 10b).

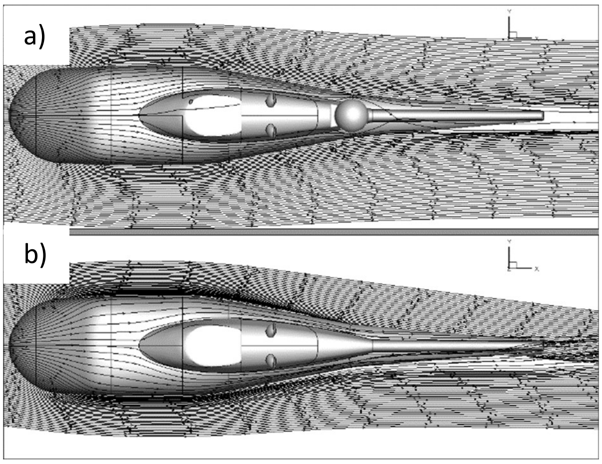

Figure 10: Comparison of flow stream traces. Credits: PZL-Świdnik

The obtained results of changes in aerodynamic characteristics (c_L, c_D, c_m) will be used in the assessment of flight performance characteristics and control margins. The issues are presented in more detail below.

The next stage of lay-up verification is the assessment of temperature distribution on the antenna radome. Due to the fact that the supporting structure of the SATCOM system must have mechanical properties ensuring adequate permeability of signal waves, due to its location on the structure of the helicopter, it should ensure adequate resistance to thermal loads and vibrations. The safety assessment was carried out on the basis of thermal analyzes based on the helicopter ground test and CFD model. In order to more accurately represent the ambient conditions, the influence of the rotor as well as the gas dynamics of the engine exhaust gas was taken into account. The reference values adopted for the analyzes are presented in table 1 below.

Table 1: Reference values used for calculated aerodynamic characteristic.

Name of parameters	Value/units
Main rotor Area	63.61[m^2]
Density (ISA)	1.209[kg/m^3]
Enthalpy	289994.5[J/kg]
Length	1[m]
Pressure	99992.27[Pa]
Temperature (ISA)	287[K]
Velocity	55.8[m/s]
Specific heat coefficient	1.4[-]
Viscosity	1.789E-05[kg/ms]

Table 2: Reference value used for calculated rotor interference.

Name of parameters	Value/units
Main rotor Area	63.61 [m^2]
Rotor radius	4.5 [m]
Rotor speed	450 [rpm] (103%)
Thrust coefficient	0.00505 [-]
Pressure	99992.27[Pa]
Pitch moment coefficient	0 [-]
Roll moment coefficient	0 [-]
Turbulence model	SAS
Number of blade	3 [-]

Mapping of the rotor operation was carried out based on CFD analyzes with additional VBM algorithms. The rotor reference parameters are presented in Table 2.

Based on the reference values adopted (Table 2) and the assumed boundary conditions values corresponding to the free-stream speed TAS = 0.3Ma, assumptions describing the characteristic cases of the β-side slip angles and α angles of attack the air flow relative to the fuselage, were defined and present on fig. 11. Numerical analyzes defining the basic aerodynamic characteristics as well as load variability are determined based on the base model as well as its modifications taking into account the EFS system. Comparative analysis of the above cases will allow to determine the impact of interference turbulence generated by EFS on the value of aerodynamic coefficients.

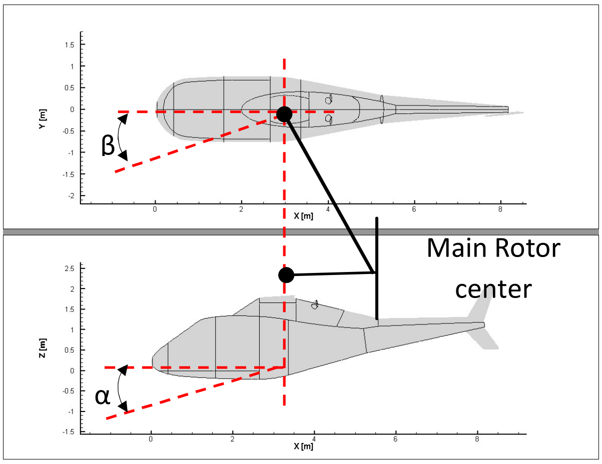

Figure 11: Assumption parameters of CFD analysis. Credits: PZL-Świdnik

For CFD analysis, Density-Based solver, computing governing equations of continuity and momentum were used along with a standard SST K-ω type turbulence model with additional energy equations. The air model was described as the Ideal-Gas with the Sutherland three-parameter model of viscosity.

The boundary conditions were defined by the Pressure Far-Field model, where parameters such as the speed of incoming air, inflow angle, static pressure (stagnation), ambient temperature parameters according to ISA atmosphere dependencies and in accordance with the following equations (1)(2) were determined. Values of carrier forces Cl and resistance forces Cd are determined for reference parameters values specified in Table 1. The values of aerodynamic moments Cm-x, Cm-y, Cm-z are determined in relation to the center of the hub (Fig. 11). The following equations describe the assumed relationship between the stagnation pressure and the ambient pressure of the tested object:

(1) $$\frac{p_o}{p} = \left[1 + \left(\frac{\gamma - 1}{2}\right)M^2\right]^{\frac{\gamma}{\gamma-1}}$$

(2) $$\frac{T_0}{T} = 1 + \left(\frac{\gamma - 1}{2}\right)M^2$$

Where:

P_0	reference pressure 101325[Pa]
T_0	reference temperature 288[K]
γ	gas constant
M	Mach number

The visualization of the induced speed (hover condition) distribution for the helicopter configuration with the active EFS system and SATCOM antenna is shown in Figure 12.

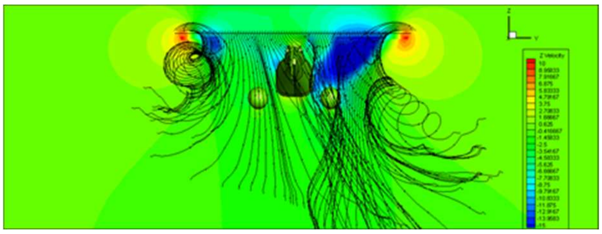

Figure 12: SW-4 SOLO Induced velocity plot. Credits: PZL-Świdnik

In order to verify the temperature distribution on the antenna radome, the numerical model of the helicopter was supplemented with additional boundary conditions simulating the gas-dynamic state of the engine. Table 3 shows the basic gas-dynamic parameters according to the manufacturer's data and presented in the IDM, depending on the power and ambient conditions.

Table 3: Definition of parameters for mass output determination.

Engine Power	Air flux lbs/s	Fuel flux lbs/s	Temp ^{0}C
85% MCP	3.2	230	700
100 %MPC	3.6	260	815

The integration of the numerical model was performed in the Ansys Fluent environment. The numerical model of the helicopter structure is adapted to assess the distribution of the temperature and pressure field depending on the flight phase. The analysis strategy of the plant firstly validates the results based on tests on a real object. Figures 13 and 14 below show the visualization of the SW-4 SOLO helicopter in the configuration dedicated to temperature measurements on the SATCOM antenna radome.

Figure 13: Antenna installation – general view. Credits: PZL-Świdnik

Figure 14: Antenna installation – right and left side view. Credits: PZL-Świdnik

Having the results on the temperature level on individual measuring sensors, the procedure of fine-tuning the computational model was carried out (Fig. 15) in order to obtain the highest possible compliance at specific measurement points. The measurement system assumes the use of thermistors glued on the side surface of the antenna (self-adhesive thermos strips).

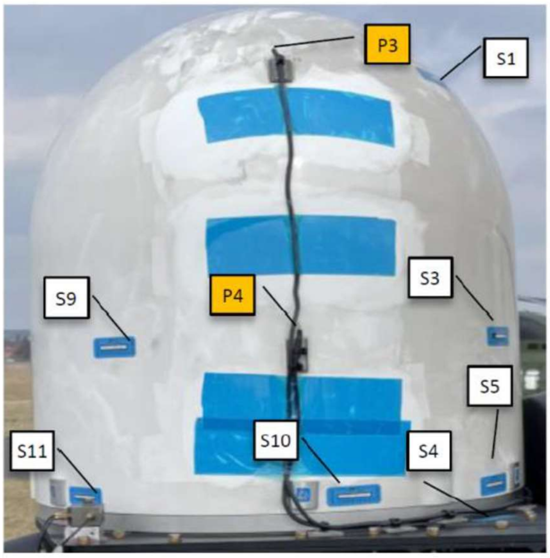

Figure 15: Temperature sensor (yellow boxes – termocouples, white boxes – thermo strips) Credits: PZL-Świdnik

The use of passive thermistors will determine the maximum temperature in places potentially most exposed to thermal loads. In addition, in areas most exposed to the effects of hot gases, thermal sensors have been installed to allow continuous temperature measurement (thermocouples).

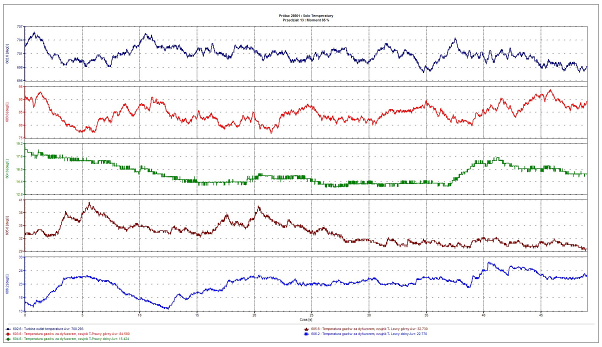

Figure 16: Visualization of temperature course at measuring points. Credits: PZL-Świdnik

Table 4 below presents the values of average and maximum temperatures determined on the basis of analyzes of time courses of individual sensors, measured on a real object.

Table 4: Temperature levels during test [3]

Measuring point	Avg [^{0}C]	Avg [^{0}C]
602.6	700.2	705.4
603.6	84.5	92.3
604.6	15.4	18.5
605.6	32.7	39.7
606.6	22.7	30.7

The final result of the numerical analyzes of the SW-4 SOLO helicopter model, tuned in accordance with the data obtained from ground tests, is shown in Figure 17 below.

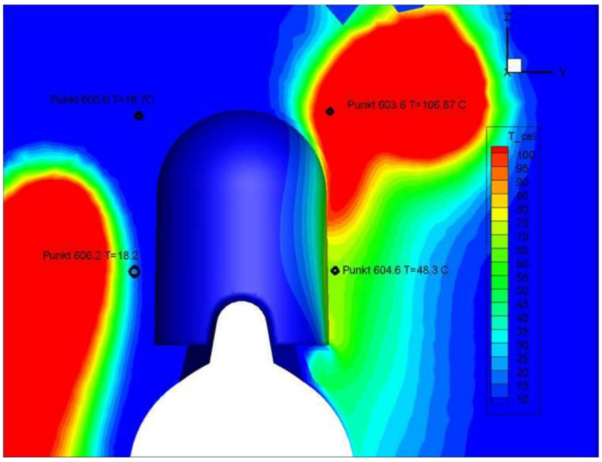

Figure 17: Visualization of the temperature distribution on the antenna structure for the case of hover, directly probe from CFD analysis. Credits: PZL-Świdnik

With numerical analyzes allowing to determine the maximum temperatures with an accuracy of ΔT=5^{0}C, the envelope of the states for which the verification was carried out was extended in order to eliminate the potential danger of damage to the fairing, which could result in detachment from the mounting points and hitting the tail rotor or the main rotor. Fig. 16 shows the visualization of the temperature field determined for the level flight condition with the forward speed TAS = 100 kts.

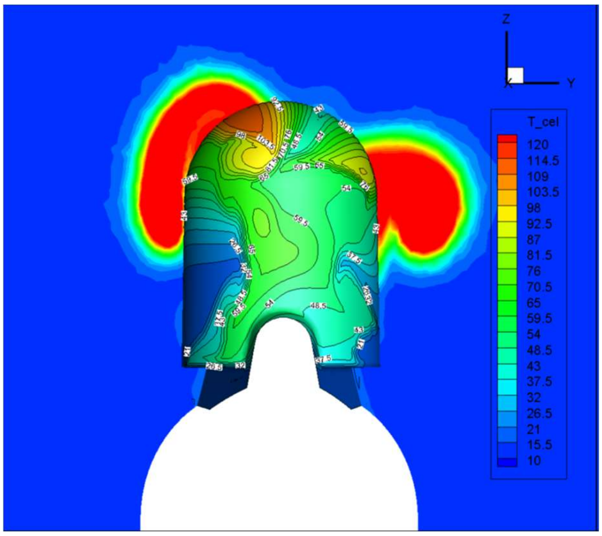

Figure 18: Visualization of the temperature distribution on the antenna structure for the caser of horizontal flight with a speed of 100kts. Credits: PZL-Świdnik

Having aerodynamic loads, pressure distributions on the antenna radome were determined. The adopted calculation conditions assume flight at the speed of TAS=1.11Vne at the lowest operating temperatures. The obtained load values will be used as a boundary condition in subsequent calculation loops defining both static and fatigue strength (more fully explained in Static strength and fatigue evaluation). The visualization of the distribution of aerodynamic loads is shown in Figure 19 below.

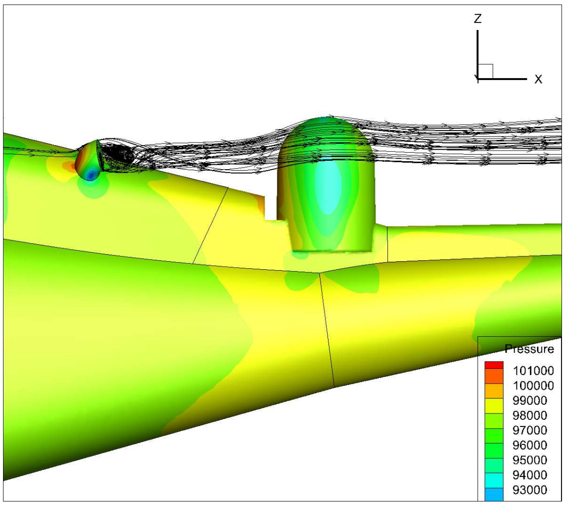

Figure 19: Visualization of pressure distribution on helicopter fuselage. Credits: PZL-Świdnik

3.3. Static strength and fatigue evaluation

3.3.1. Emergency Floatation System mounting

The subject of analysis was provision for installation of EMSA floatation system on the SW-4 SOLO landing gear skids. The objective of analysis was to determine static strength of the floatation system mounting elements and the landing gear for in-flight cases and normal landings and to provide evidences for supporting clearance to an experimental permit to fly acc. to Joint Aviation Regulations JAR 27 (with amendment 27/98/1). In the analysis the in-flight loads (mass forces and aerodynamic) and landing loads (related with the speed of contact with ground) of packed and inflated floats were considered and their influence onto the skid and brackets structure. Calculations were made by the Finite Element Method with the use of Symulia Abaqus software.

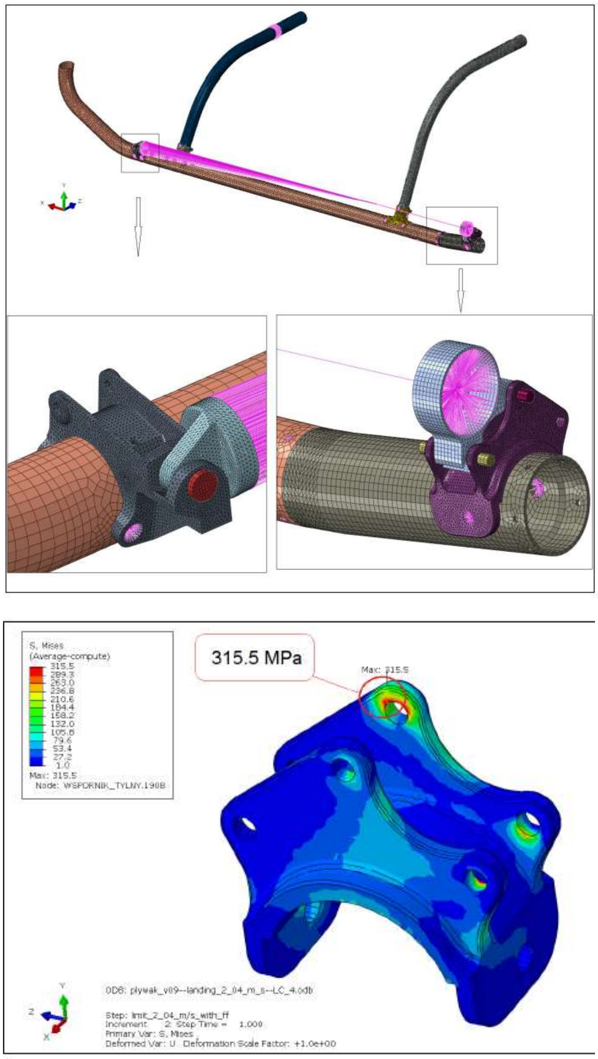

Figure 20: Floatation system mounting, FEM. Credits: PZL-Świdnik

The analysis has demonstrated sufficient static strength of floatation system mounting to the skid landing gear. Due to symmetry of landing gear structure, only its left half with the LH float mounting elements were modelled. Landing gear legs, the skid, fittings of the skid mounting to the leg and elements of floatation system mounting to the landing gear were modelled with the use of solid elements. Beam elements and “coupling-kinematic” - type elements were used to model fittings. Contact impact between the model elements was also taken into account. A node corresponding to the CG of the float, to which loads were applied were joined with the forward and the rear lug of float mounting with the use of “coupling-kinematic”-type element. The following scenarios were investigated:

- in-flight loads for packed floats for selected in-flight cases - application of mass forces to the center of mass of packed floats for in-flight cases according to the methodology for determining loads for the SW-4 SOLO loads; aerodynamic loads for V_{NE} and minimum temperature at H=0m added to determined mass loads;
- in-flight loads for fully inflated floats - application of mass forces with acceleration 2g directed downwards to the center of mass of floats; jointly with a mass load, an aerodynamic load applied in the geometric center of cylinders acts;

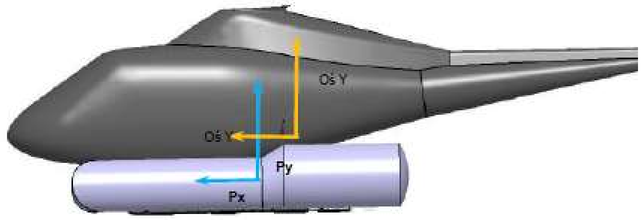

Figure 20: Position of coordinate systems for inflated floats. Credits PZL-Świdnik

- inertial loads of floats mounting during landing (packed float) - based on calculation of rigidity of nodes for the center of gravity it can be assumed that the reactive force for a single float depends linearly on the speed of contact with the ground; the force is applied in CG of packed floats;

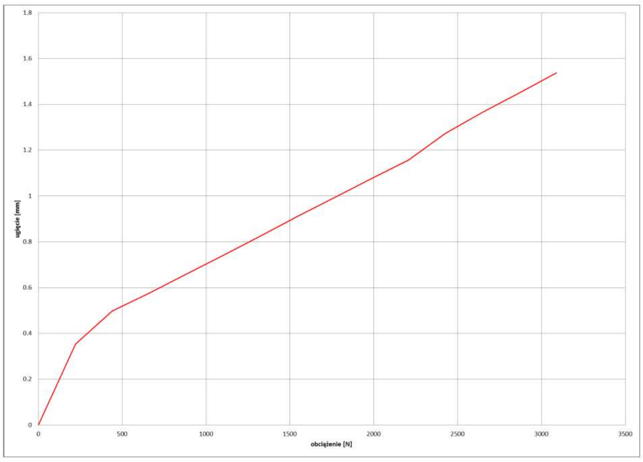

Figure 21: Dependence of deflection of packed float’s center of mass on force applied in the center of mass. Credits: PZL-Świdnik

- inertial loads of floats mounting during landing (inflated float) - based on documentation of floatation system it was assumed that the total mass of one float is divided into a metal shield and an inflated part 50% each.

Total vertical force is a sum of forces coming from the shield acting in the center of mass of the shield and the float’s inflated part acting in the center of mass of inflated floats.

The rigidity of deflection of the float’s inflated part was determined; calculation results are presented in figure below.

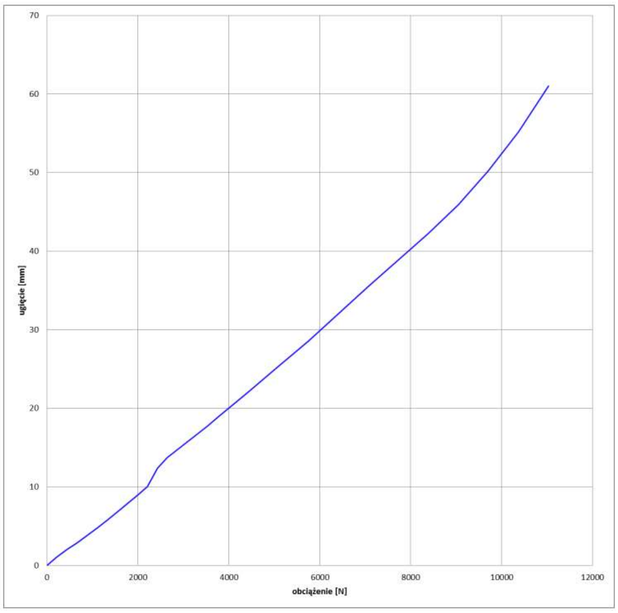

Figure 22: Dependence of deflection of inflated float’s center of mass on force applied in the center of mass. Credits: PZL-Świdnik

The following step was to perform static strength analysis for the mounting of floatation system inflation cylinders.

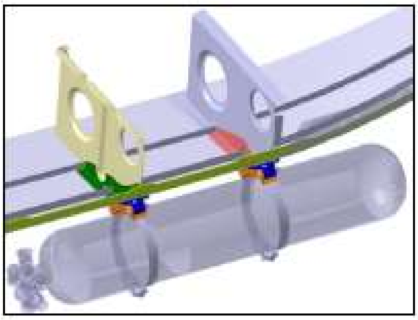

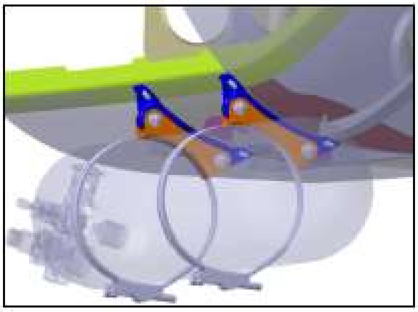

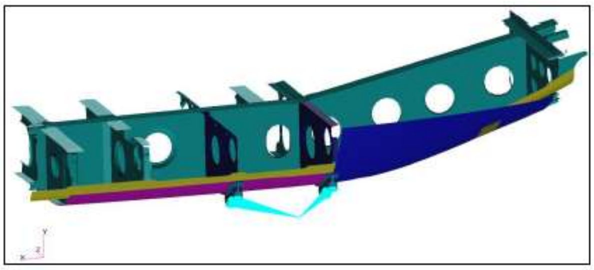

Figure 23: Mounting of floatation system inflation cylinders. Credits: PZL-Świdnik

The subject of analysis was the provision for mounting of the floatation system cylinders on the fuselage structure (area between frame no. 8 and 9) of the SW-4 SOLO helicopter. All cases of loads in flight and the cases of normal landing were analyzed, apart from the case of crash landing.

Calculations were made using Nastran 2014 SOL 101 software using FEM. The analysis has shown sufficient static strength of the provision for the floatation system cylinders mounting on the SW-4 SOLO helicopter fuselage structure.

The mass of floatation system cylinder mounting and assembly elements was implemented in the FEM model through the density of materials and the volume of particular elements.

3.3.2 SATCOM

Besides the confirmation of performance characteristics of the helicopter in new configuration, static and fatigue analyzes have been prepared as well, to ensure safety of operation from structural point of view. The subject of analyses were the provision elements for: the SATCOM system installation together with the adjacent fuselage structure and radome installation.

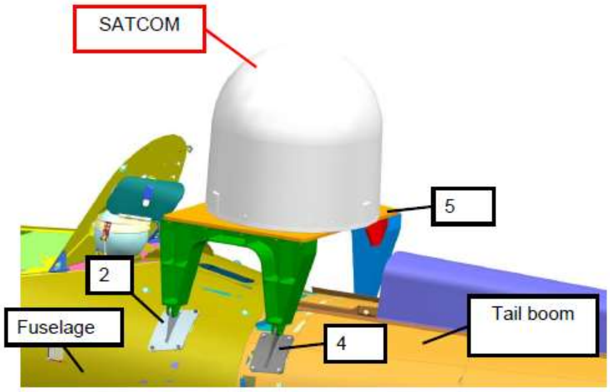

Figure 24: The SATCOM system installation together with the adjacent fuselage structure. Credits: PZL-Świdnik

For the structure strength analysis, the aerodynamic force acting on system was simplified as aerodynamic drag force oriented through axis with direction opposite to the h/c flight velocity. Force was determined as the drag of cylinder with spherical end under the air stream (the induced velocity from MR source is added to the free stream velocity), flown perpendicular to the cylinder axis.

For radome strength analysis aerodynamic loads were used as a distribution of the pressure loads over the SATCOM radome applicable. The distribution was based on the results of CFD calculations.

The calculation model is based on a simplified 3D model of the helicopter with the modification of the fuselage structure taking into account the installation of the SATCOM antenna.

The analyses were made with the consideration of the FAIL-SAFE approach. For that situation destruction of the limiting bolt in each of the system's installations elements were simulated by removing elements modelling the bolt from the FEM analysis.

The analyses were made with the consideration of the FAIL-SAFE approach. For that situation destruction of the limiting bolt in each of the system's installations elements were simulated by removing elements modelling the bolt from the FEM analysis.

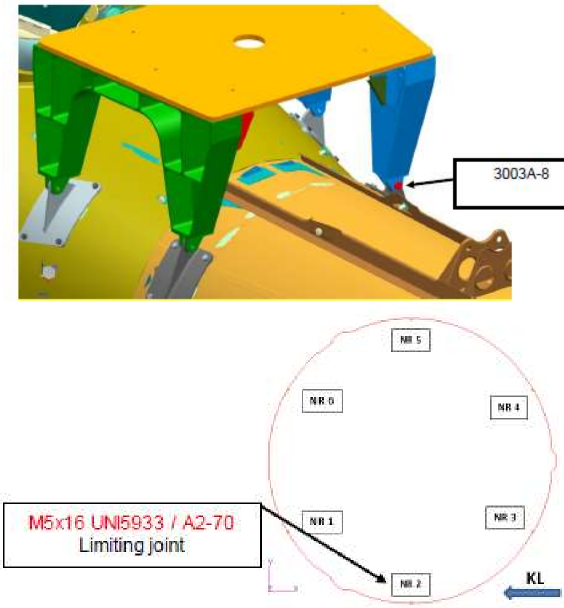

Figure 26: Limitation bolts for FAIL-SAFE analysis. Credits: PZL-Świdnik

All load cases in flight and during normal landings were considered. Based on the analysis of calculation results of the limit load factors in flight and during landing (excluding emergency landing cases), the limiting load cases were selected to cover all flight load cases in flight and during normal landings consist of aerodynamic and inertia forces.

The subject fatigue of analyses were the provision elements for:

- the SATCOM system installation together with the adjacent fuselage structure;
- the system antenna radome installation.

The fatigue life was determined for the in-flight variable stresses of the SATCOM system mounts to set the guaranteed fatigue lives of SATCOM installation elements. To determine the fatigue life, the S-N material curves derived from fatigue tests of material specimens were used.
Fatigue loads were determined from accelerations at the installation points of the SATCOM system to the fuselage structure. First set of loads comes from helicopter structure vibration and have to be applied as kinematic excitation of the support to fuselage connection points. The second loads set comes from aerodynamic pressure pulsation due to MR blades passage over the SATCOM antenna radome and then variation of the induced velocity.

The accelerations originating from the fuselage were applied to four attachment points of the SATCOM system to the fuselage structure. The variable force originating from the MR blades was applied as a concentrated force at the center of gravity of the SATCOM system antenna and distributed to the attachment points modelling the antenna cover using the MPC RBE-3 element.

The conservative approach was used for the fatigue life analyses using assumption that maximum values of determined vibration amplitudes are used for full spectrum of the flight envelope.

4. PERFORMANCE & FLIGHT MECHANICS

4.1. General

Installation of external equipment affects helicopter performance and flight mechanics in terms of control margins, static and dynamic stability. Moreover, time dependent aerodynamics devices, as Emergency Floatation System, requires dynamic response investigation. All of mentioned analyses are covered by set of CAE tools employed in PZL. They include basically FORTRAN based in-house software OSW4, DDSSW4, O50, O44R.

In line with these, state-of-the-art commercial software FLIGHTLAB was employed, to support unsteady or unsymmetrical flight state analysis. In addition to numerical calculation, a comprehensive maritime simulation environment was established. It integrates FLIGHTLAB simulation engine, navy vessel dynamics and aerodynamics as well as external conditions, as presented by Topczewski et al. (Ref. 2). The environment is implemented on simulator hardware consisting of SW-4 SOLO cabin and display suite, shown in Figure 27. Thanks to this asset, computational analyses were significantly validated and maritime mission safety evaluated with high fidelity. Ref. 3 and 4 discuss HMI study on pilot's performance and workload based on the simulator.

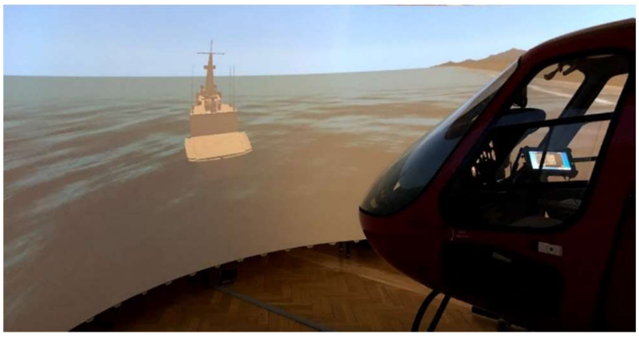

Figure 27: Overview of SW-4 SOLO simulator. Credits: Warsaw University of Technology

Computation and simulation analyses are necessary at the early stage before permit-to-flight is issued. Then flight test trials are conducted to validate these and confirm operational safety. Following chapters present methodology adopted for each discipline for both project. Figure 28 shows general analysis framework concept, emphasizing flight test validation loop.

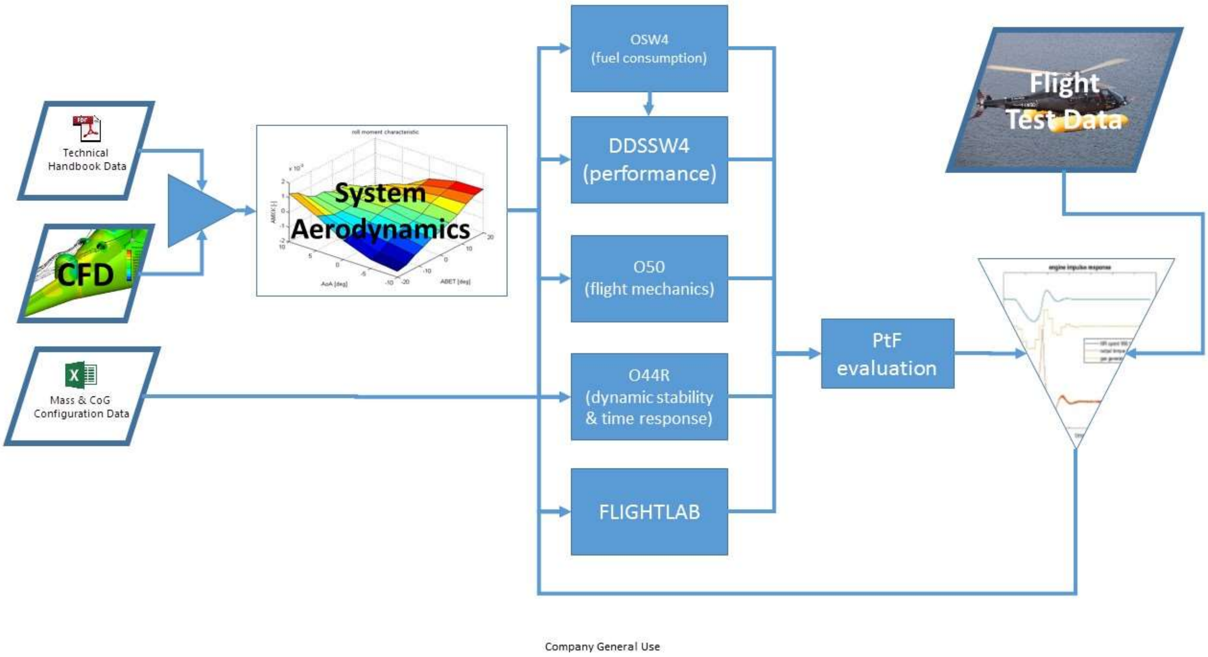

Figure 28: Performance and flight mechanics analysis framework. Credits: PZL-Świdnik

4.2. Input data

To evaluate helicopter performance and flight mechanics, helicopter baseline model established for SW-4 SOLO should be supplemented with external equipment aerodynamics and weight & balance.

For simple shapes, common handbook data based on wind tunnel tests is employed, as shown in Ref. 1. This approach is strictly limited to applications not affected by the aforementioned flow phenomena:

1. complex and turbulent flow around rear part of fuselage;
2. strong interferences of rotors and stabilizers;
3. main rotor downwash.

These limitations imply that handbook data could be employed for forward level flight conditions at speed above transition effect threshold. For SW-4 SOLO baseline the threshold speed is 40km/h, as indicated in red in Figure 29. It can be noticed that the transition effect limit corresponds well with power curve inflexion point.

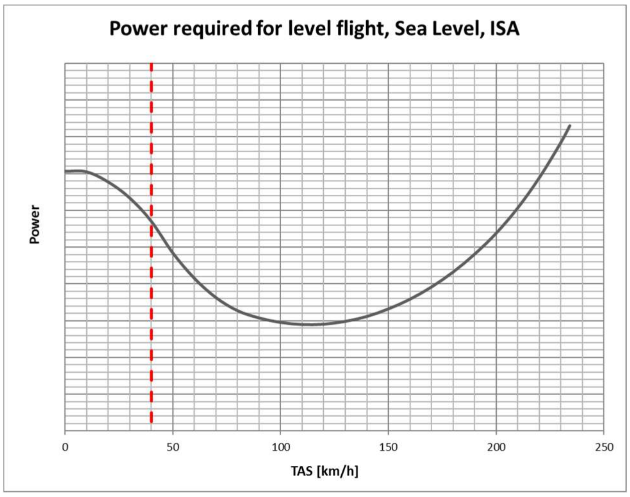

Figure 29: Power required for level flight. Credits: PZL-Świdnik

In addition to that, handbook data aerodynamics could be applied to forward or skid mounted equipment, where flow is undisturbed (close to far field conditions). These assumption are met for optoelectronic head, radar array and EFS in OCEAN2020 configuration, as shown in red in Figure 30.

SATCOM antenna, which is the main component of RPAS In Air configuration, is installed in highly turbulent region at tail boom root, where strong interferences and main rotor downwash is present. In such conditions, CFD analysis was the base for aerodynamic characteristics.

Floats in inflated state are closer to the fuselage therefore more affected by its interference. To assess this influence both aerodynamic approaches were used. Handbook based data allowed significantly faster calculation time. On the other hand, CFD based data is more accurate and allowed to simulate helicopter behavior in wider range of inflow angles.

Figure 30: SW-4 SOLO in OCEAN2020 configuration. Credits: PZL-Świdnik

Figure 31: SW-4 SOLO in RPAS In Air configuration. Credits: PZL-Świdnik

In case of PZL in-house software (OSW4, O50, O44R) external equipment aerodynamics was implemented as addition to baseline fuselage characteristics after rescaling by the reference area and length in accordance with the Eq. (1)-(3). Pitching and yawing moment coefficients were derived from drag and corresponding arm. Impact on rolling moment was neglected.

(3) $$C_{d,total} = C_{d,base} + C_{d,equip}\frac{S_{equip}}{S_{base}}$$

(4) $$C_{p,total} = C_{p,base} + C_{p,equip}\frac{S_{equip}l_{equip}}{S_{base}l_{base}}$$

(5) $$C_{y,total} = C_{y,base} + C_{y,equip}\frac{S_{equip}l_{equip}}{S_{base}l_{base}}$$

FLIGHTLAB modelling system allows flexibility in input data definition. Thus, both handbook and CFD based aerodynamic data sets were provided for EFS. These two modelling strategies were investigated in scope of HELIMARIS project, which was proceeded in line of OCEAN2020.

4.3. Performance

Helicopter performance is of main interest while any external equipment is concerned. It should be assessed to ensure meeting expected operational capabilities of the SOLO system. This is vital especially in maritime operation scenario as tested in scope of OCEAN2020 project.

Based on a system aerodynamics defined, OSW4 FORTRAN code was employed. Program performs helicopter trim for given conditions and configuration. Then, it evaluates total power required for level flight and fuel consumption in function of TAS for various TOW, H_p and OAT. Figure 32 presents calculation results for each analyzed configuration. Parasite drag of SATCOM antenna resulted in significant deterioration of level flight limits. Both V_H speed corresponding to MCP limit and V_{MAX} corresponding to TOP limit deteriorated by approximately 17km/h.

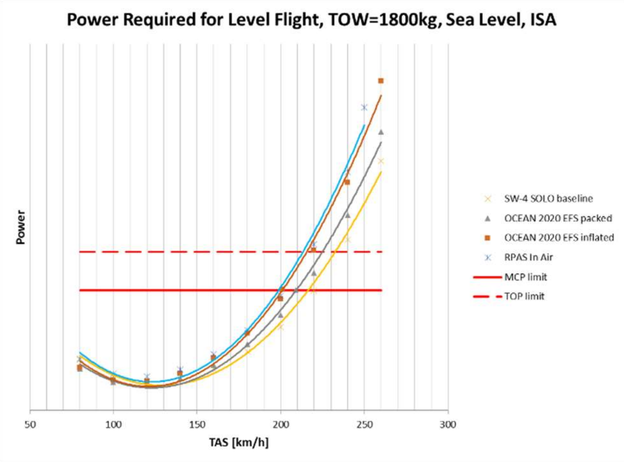

Figure 32: Speed limitations for SW-4 SOLO in both projects. Credits: PZL-Świdnik

Results obtained with use of OSW4 were then transferred to DDSSW4 and supplemented with TOW/fuel capacity defined for each particular helicopter configuration. Inputs are power required characteristics, fuel consumption, main rotor polar and engine limitations. The code evaluates basic performance in terms of hover ceiling, maximum thrust, range, endurance and maximum ROC. Not all of these were vital in scope of presented projects and required operational capabilities. In OCEAN2020, main rotor choke effect in presence of inflated EFS was taken into account. It was assumed that thrust loss is doubled due to two times larger cross section with respect to MR downwash. In RPAS In Air, only forward flight performances were taken into account, because cruising/patrol mission profile was of main interest. In Table 5, performance changes are presented for both projects. In case of change less than 1%, no change is indicated. Performances which were considered irrelevant, are marked by "-".

Each configuration analyzed was affected by external equipment installation. The main impacts were identified with respect to high speed cruise performance (V_H, range) and hover ceiling in presence of inflated floats. Despite of these deterioration, the system performance met expected mission capabilities within defined envelope.

Table 5: Basic performance evaluation.

Configuration	OCEAN2020		RPAS In Air
	EFS packed	EFS inflated	
Hover Ceiling	no change	less by approx. 200 m	-
Maximum Thrust in Hover	no change	less by approx.. 50 kg	-
ROC at MCP	less by approx. 1.6 %	less by approx. 4.7%	less by approx. 5.7 %
V_H	less by approx. 5.5 km/h (5 km/h)[a]	less by approx. 13 km/h	less by approx. 17 km/h
Range	less by approx. 3.5 % (2.8 %)[a]	less by approx. 6.7 %	less by approx. 8.9 %
Endurance	no change	less by approx. 1.7 %	less by approx. 2.3 %

[a]EFS only

4.4. Control margins

External equipment installed at long distance from helicopter CoG could significantly affect its equilibrium due to changed fuselage attitudes (pitch, roll, yaw). Another case is main rotor downwash choke effect in hover due to significantly larger cross-section. In scope of presented projects, EFS is the main concern. Therefore, control margins were checked for OCEAN2020 project configuration.

O50 FORTRAN code is used to evaluate helicopter control trim for equilibrium conditions. Level flight with TOW=1800kg at sea level in ISA was assessed. Limiting aft position of CoG is critical for SW-4 SOLO with respect to control margins. Two speeds were considered:

- V_{NE} for the assumed conditions;
- 110km/h – assumed cruising speed for operational scenario.

Table 6 shows change of swashplate pitch and TR pitch trimming, relative to control range. As noticed in Table 5, change of less than 1% was neglected. This applies to cruise speed. At V_{NE} control margins deterioration becomes relevant, but still does not affect safety. These conclusions were confirmed during flight test campaign.

Table 6: Control margins change in OCEAN2020 configuration.

Control channel	Swashplate Pitch	TR Pitch
TAS=110km/h		
EFS packed	No change	No change
EFS inflated	No change	No change
TAS=V_{NE}		
EFS packed	-1.3 %	-1.8 %
EFS inflated	-3.8 %	-4.8 %

4.5. Static stability

Similarly to control margins, static stability of the helicopter is also affected by installation of any external equipment. Applicable certification standards require to check two control channels: swashplate pitch (longitudinal static stability) and TR pitch (directional static stability).

It is defined that helicopter is statically stable when control change in particular channel implies an unambiguous response of corresponding attitude. In terms of longitudinal channel, the sign of derivative of MR swashplate pitch with respect to helicopter pitch should be positive when pitched in both directions. In terms of directional channel, the sign of derivative of TR pitch with respect to helicopter sideslip should be positive when yawed in both directions. MR collective is fixed.

RPAS In Air configuration was found to be vulnerable to static stability deterioration due to mission profile assuming long cruising and maneuvers with SATCOM antenna. Again, O50 code was employed to calculate equilibrium and control attitudes. Calculations were made for helicopter configuration same as for control margins evaluation. Maximum level flight speed V_{MAX}=218km/h was considered. Due to O50 trimming limitations, quasi-fixed MR collective approach was adopted by applying fixed power. The system was found to be statically stable in both channels, since the derivative conditions are met. Figure 33 presents evaluated derivative values for directional static stability.

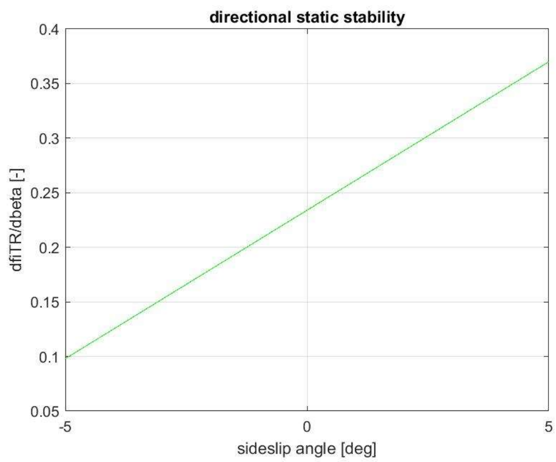

Figure 33: Directional static stability for RPAS In Air configuration. Credits: PZL-Świdnik

4.6. Dynamic stability

Dynamic stability indicates if system reaction amplitude decline or arise over time, after any control variable or conditions are perturbed. Moreover, two basic regimes of response are distinguished: oscillatory and aperiodic. It is a fundamental feature of aircraft affecting practical handling qualities and operational safety. It applies particularly to helicopters, when unsteady aerodynamics and strong interferences are present. Dynamics identification is important when designing AFCS and SAS systems which are widely employed to handle flight perturbances, reduce pilot workload and improve operational capabilities. That is main scope of SW-4 SOLO development, investigated during several flight test campaigns and research projects. Reference 2 presents preliminary AFCS study with emphasis on maritime operation.

Classical stability theory is described by De Silva (Ref. 5). It is based on dynamic model linearization around the equilibrium state. Classical stability parameters (eigenvalues, oscillation period, doubled/half-amplitude time) are derived from characteristic equation solution. System is considered as stable when eigenvalue real part is negative. The theory is implemented in O44R code.

In OCEAN2020 project, oscillation period and double/half-amplitude time was calculated in function of TAS for various balancing, TOW=1650kg and H_p=500m. Figure 34 shows that stability of the system increases with flight speed. Oscillation period T vary slightly within analyzed speed range, while double-amplitude time t_2 increases significantly above 20km/h. The reasons of that are mainly higher efficiency of stabilizers and decreasing interference between fuselage and rotors. It can be noted that extreme aft position of CoG is critical, which justifies assumptions made.

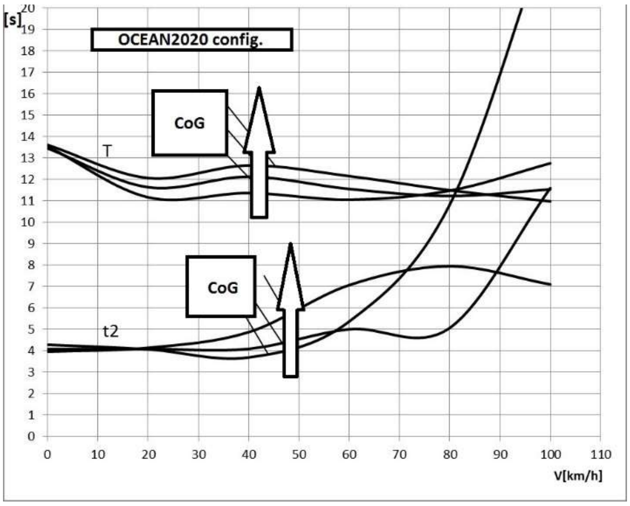

Figure 34: Dynamic stability of OCEAN2020 configuration. Credits: PZL-Świdnik

In RPAS In Air project, classical dynamic stability was assessed for high speed conditions. Configuration assumed was the same as for static stability, while level flight on H_P=1km in ISA conditions with corresponding V_{NE} considered. Results in Table 7 shows satisfactory dynamic behavior of the system. Almost every eigenvalue has negative real part, which indicates stable (damped) motion. Single eigenvalue with positive real part has doubled-amplitude time long enough for pilot to easily maintain control over the helicopter.

Table 7: Dynamic stability of RPAS In Air configuration.

Eigenvalue real part	Eigenvalue imaginary part	Oscillation period	Doubled/Half-amplitude time
-0.9127	4.3013*I	1.4608 s	0.7595 s
-0.9127	-4.3013*I	1.4608 s	0.7595 s
-1.5023	1.4394*I	4.3651 s	0.4614 s
-1.5023	-1.4394*I	4.3651 s	0.4614 s
-1.7944	0.0000*I	Aperiodic motion	0.3863 s
-0.0383	0.2414*I	26.0291 s	18.0950 s
-0.0383	-0.2414*I	26.0291 s	18.0950 s
0.0424	0.0000*I	Aperiodic motion	16.3344 s

4.7. Dynamic response

Installation of Emergency Floatation System required analysis of unintentional inflation of one and both of the floats. This case was identified as one of potentially hazardous, thus it is necessary to confirm if AFCS or pilot on-board could maintain controllability and continue safe operation. To asses impact of floats inflation, aerodynamic characteristics of them were provided as described in Chapter 4.2. It was assumed that transition between packed and inflated state is linear. Inflation time was provided by EFS manufacturer and confirmed by ground tests.

Firstly, analysis were made with use of PZL in-house software. O44R code was used to calculate complete matrix of derivatives of linearized model state parameters with respect to perturbances. Than IMPA code was employed to simulate helicopter time response for various control reaction delays. Both floats inflation and unsymmetrical cases were analyzed. Critical helicopter configuration was established by dynamic stability analysis in Chapter 4.6. Flight perturbation in terms of Euler angles for V_{NE} case is shown in Figure 35. Presented results are for 3s control delay which is the most profound case for controllability and safety check. For symmetrical and left-side inflation, attitudes perturbation does not exceed 15°. The worst configuration is right-side unsymmetrical when yaw and roll angles perturbation arises up to 20° and 50° correspondingly. This asymmetry between left and right-side inflation is coming from fuselage aerodynamic characteristics and MR rotation direction. In every analyzed case, helicopter controllability is maintained, even after 3s delay of SAS/pilot reaction. Moreover SAS was assumed to have only 18% of authority for this study.

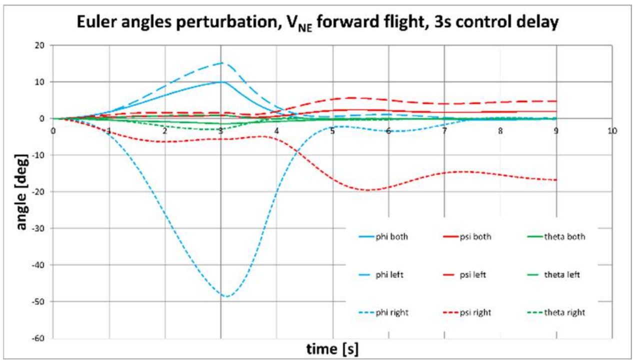

Figure 35: Dynamic response in case of EFS inflation. Credits: PZL-Świdnik

Secondly, FLIGHTLAB based studies were carried out. This activities were performed in cooperation with Warsaw University of Technology in scope of HELIMARIS project. Żugaj et al. (Ref. 6) presents detailed study on AFCS/SAS system assumptions, performances and robustness in different scenarios. Two aerodynamic models were employed as described in Chapter 4.2. Model 1 is based on handbook aerodynamic data while model 2 on CFD results. Following Figures 36-39 show dynamic response for various AFCS/SAS modes and time delays. MTOW and medium balancing was considered, ISA conditions at H_P= 600m (2000ft) and cruise speed TAS=204km/h (110kts). Data legend is as follows:

- dark blue – AFCS/SAS disengaged,
- green – AFCS/SAS engaged without delay,
- violet – AFCS/SAS engaged with 1s delay,
- light blue – AFCS/SAS engaged with 3s delay.

In this study, only 10% of SAS authority was assumed while AFCS of full range of control. Only symmetrical inflation case was simulated. It can be noticed that SAS with 10% authority is not capable of reducing the perturbances. Model 2 is less stable. Conclusions are that wider range of given authority could ensure controllability and safety even in case of 3s delay.

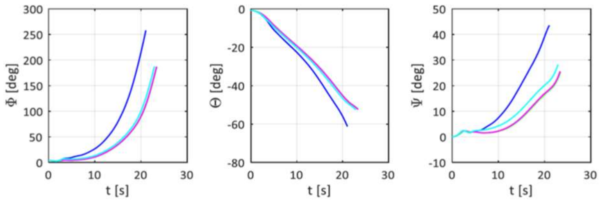

Figure *36*: Dynamic response for model 1, SAS only. Credits: PZL-Świdnik/WUT

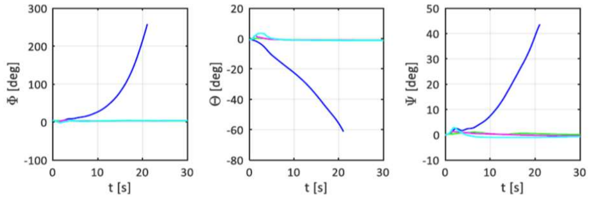

Figure *37*: Dynamic response for model 1, AFCS. Credits: PZL-Świdnik/WUT

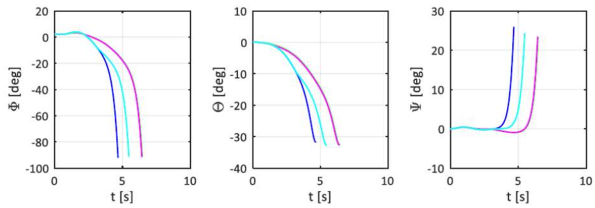

Figure 38: Dynamic response for model 2, SAS only. Credits: PZL-Świdnik/WUT

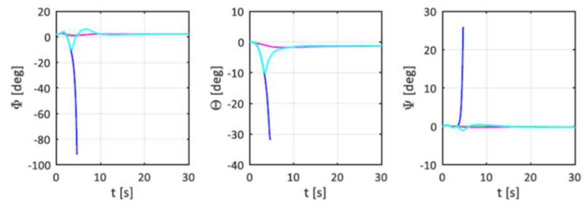

Figure 39: Dynamic response for model 2, AFCS. Credits: PZL-Świdnik/WUT

Helicopter dynamic response in case of EFS inflation was further tested during simulator test campaign employing PZL test pilots. Figure 40 below shows attitudes perturbation assuming no delay of pilot reaction for symmetrical inflation. EFS inflation start is marked with dashed line. Configuration, TAS and flight conditions were the same as for numerical analyses in the previous stage. Simulator tests confirmed that pilot acting with full authority and control range can easily maintain controllability and continue flight.

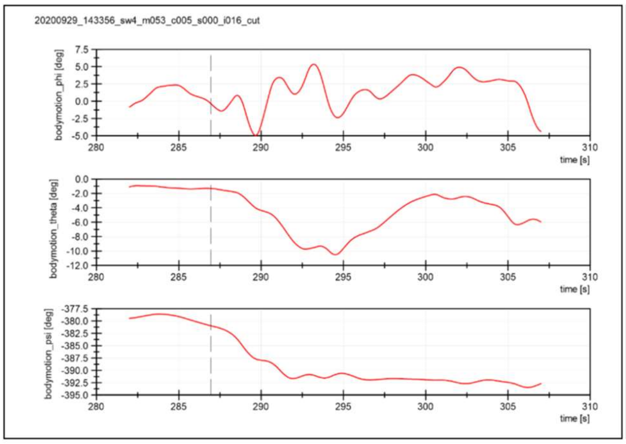

Figure 40: Simulator test of EFS inflation. Credits: PZL-Świdnik/WUT

Finally, system safety in case of unintentional EFS activation was evaluated in flight test campaign.

5. GROUND AND FLIGHT TESTS

5.1. Emergency Floatation System

The test purpose was to obtain evidence of compliance required to approve the SW-4 SOLO helicopter defined with the installation of Emergency Flotation System to conduct flights with a safety pilot and a flight engineer over water. As the next milestone to be completed was to provide evidence to confirm the indicators of Helimaris project (within the scope of validation of a new procedure to approach landing on a vessel).

Prior to start of flight test, the ground test phase were conducted covering evaluation of the EFS with floats stowed/deployed, check of emergency aircrew evacuation and modal tests of the EFS components. Given that all the ground activities were performed with positive results, flight test activity could start. As to ensure proper safety of flight test activity, each flight scenario were conducted starting from the easiest on, in configuration with floats stowed. These flight tests confirmed that the level of vibration amplitudes in test points not exceed the values specified in the installation requirements thus providing confirmation on the proper EFS installation aspects.

As the next point of flight activity, was to perform measurements flight with floats inflated symmetrically were both floats was inflated on ground. Together with positive opinion of an Experimental Pilot and Flight Test Engineer, during flight any unexpected behavior of inflated floats in all flight states were not observed or registered – Figure 41.

Figure 41: SW-4 SOLO with floats inflated in flight. Credits: PZL-Świdnik

The final two stages of an SW-4 SOLO activity in EFS configuration was concerned on the flight test scenario with floats inflation in flight and to evaluate helicopter behavior during approach and hover over the moving platform in additional configuration with anchor mock-up device – Figure 42.

Figure 42: Moving platform to simulate SW-4 SOLO landing scenarios on vessel. Credits: PZL-Świdnik

During the stage of flight tests with floats inflated symmetrically, after the pre-flight test procedure checking of the float system, flights were performed, under which the following aspects were assessed:

- floats inflation time,

- the process of floats inflation in level flight and the impact on pilot control, maintaining a stable flight during and after inflation of the floats,

- influence on the aerodynamic properties of the helicopter in flights with inflated floats,

- determination of the Vh speed for the helicopter with the floats inflated, with respect to the basic configuration of the helicopter,

- defining hourly fuel consumption in various configurations.

In addition, as a part of these tests, the effect of inflated floats on increasing the pitch inclination was identified, and neutral longitudinal stability characteristics were demonstrated at speeds around Vh.

The aim of the last phase of flight tests, incl. the mock-up of the anchor device installation, was to practice approaches over the moving platform and finally, when the set of landing approach simulation was conducted, landing on the moving platform were conducted as well to assess the impact of the assembly of an anchor mock-up device to ensure stable behavior of the device and the appropriate distance (safety margin) to the platform surface at touchdown – Figure 43.

Figure 43: SW-4 SOLO landing approach on the moving platform with anchor mock-up device. Credits: PZL-Świdnik

Bearing in mind the scope of the tests carried out in various configurations, the general conclusions focus on the statement that the installation of the float system on the SW-4 SOLO was correctly implemented, giving positive results from ground and flight tests, at the same time paving the way for further helicopter tests as part of the future qualification of the helicopter with Emergency Floatation System on-board.

SATCOM DATALINK

The SATCOM system, operating in Ka-Band, has been designed to allow BRLOS bidirectional transmission of data, HD video and commands between the GCS and the SOLO Helicopter. In particular, the SW-4 SOLO Helicopter telemetry data/C2 and data gathered by the on board payload, was transmitted in single hop towards the co-located flyaway antenna installed at GCS. In such scenario, the Satellite Hub was used for the signaling and the carrier's management.

The flight test activity was conducted according to a Build-up approach with several increasing risk phases in order to achieve a high level of confidence towards the final demonstration phase. After ground test conducted in Świdnik were the EMC compatibility was verified together with modal checks and acceptance test procedures, to ensure proper safety level for flight test scenarios, next stages of the activity were performed in flight with SATCOM system on-board as a part of mission system and key driver for the demonstration phase. At first, dedicated flight test with Safety Pilot on board was intended to assess FCS performances after the installation of SATCOM datalink. In this phase the SATCOM datalink was not used to control the H/C but the purpose of this flight test was to verify Automatic Flight Control System performances with the new configuration, in terms of weight, CG position and aerodynamic effects. Positive results of this tests allow to start the main purpose of tests – functionality of new SATCOM system. The flight test was intended to check that the SATCOM Datalink System is working in all the phases of flight, by monitoring its functional parameters and assessing the satellite communication, and to assess the functionality of the SATCOM Datalink in terms of:

- Helicopter C2,
- Payload C2,
- Payload datastream transmission.

The main RPAS In Air project scope was the analysis of the management of an RPAS integrated in ATM operations, in a scenario of both real and simulated traffic, taking into account also any latencies caused by the SATCOM datalink and the evaluation on how these latencies and the management of contingency procedures affect the coordination between the actors involved.

The involved ATM operations were:

- Nominal SID (Standard Instrumented Departure),
- Nominal STAR (Standard Arrival Route),
- Vectoring,
- Loss of C2.

In the scope of the RPAS In Air demonstration flights, two operational scenarios were also performed:

- in the first scenario, the task was focused on the H/C that had to observe a simulated attack (by a small boat) toward a fictitious ship. A loiter was performed in order to provide EO video of the scene and to follows the small boat up to the coast.
- in the second scenario, the objective of the task for the H/C was to provide EO video of a fictitious fire located on the land.

The execution of the demonstration flight with SAT-COM system happened within the controlled airspace class A-C.

Area of operations include the Grottaglie Test Bed Restricted Airspaces (R315, R316 and R317) - see Figure 45. R315 and R316 Areas were not segregated, while the R317 Area could be segregated. In this case, no communication with ATC was needed once the NOTAM was activated. Take-off and landing were performed in the Taranto-Grottaglie airport LIBG - Figure 44. Runway in use was agreed and selected according to ATC indications and operational limitations – Figure 46 and 47.

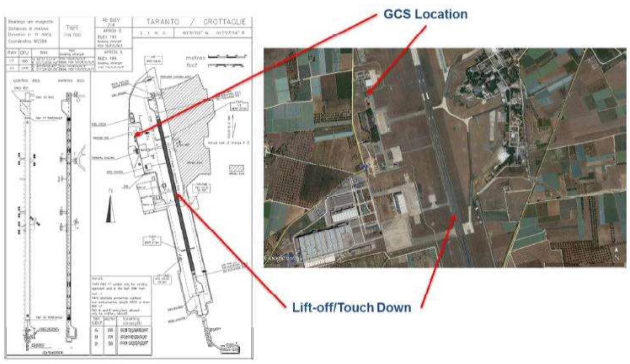

Figure 44: Taranto/Grottaglie LIBG Airport. [8]

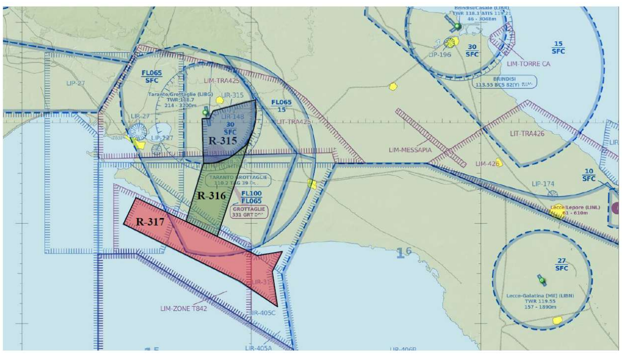

Figure 45: Grottaglie Test Bed Restricted Airspaces R315, R316 oraz R317. [8]

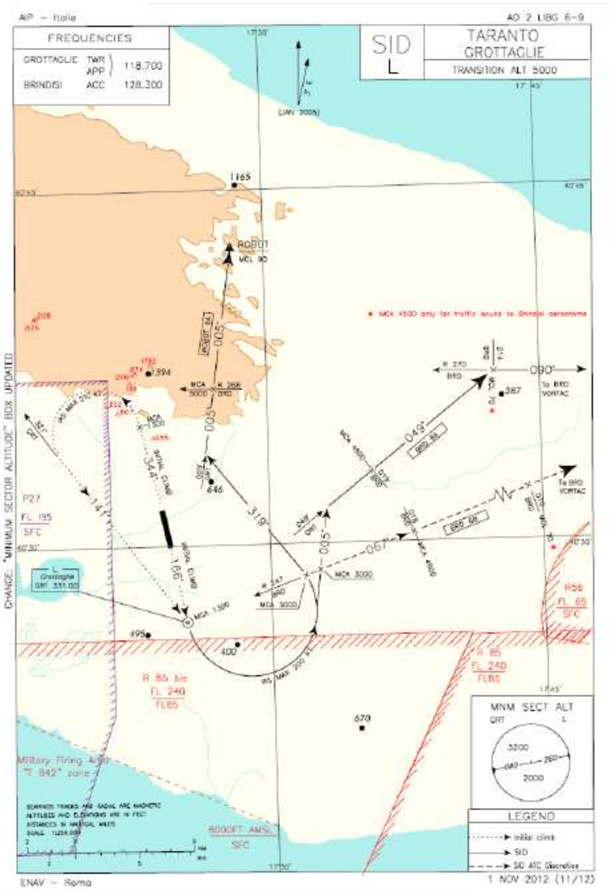

Figure 46: Standard Instrument Departure SID Map for LIBG (Grottaglie). [8]

Figure 47: Standard Terminal Arrival Route for LIBG (Grottaglie). [8]

The final demonstration flights with SATCOM system was performed under the control authority of:

- ATC Grottaglie,
- ATC Brindisi,
- ATCO (Grottaglie ENAV).

The ATCO is a simulated ATC located in Grottaglie, which gave orders to the Remote Pilot according to the real and simulated traffic that they observed in their CWP (Controller Working Position). The ATCO stand was located in the ATC Grottaglie building, voice communication between the Ground Pilot and the ENAV representative (ACTO) was provided by VoIP (Voice over IP). The safety pilot communicated with ATC Grottaglie using an on-board radio on the 118.70 MHz tower frequency. The ground pilot in GCS communicated with both ATC (via radio - 118.70 MHz) and ATCO (commands given by voice or telephone). The ground pilot was also able to communicate with the safety pilot in the SW-4 SOLO helicopter (via radio - 121.45 MHz).

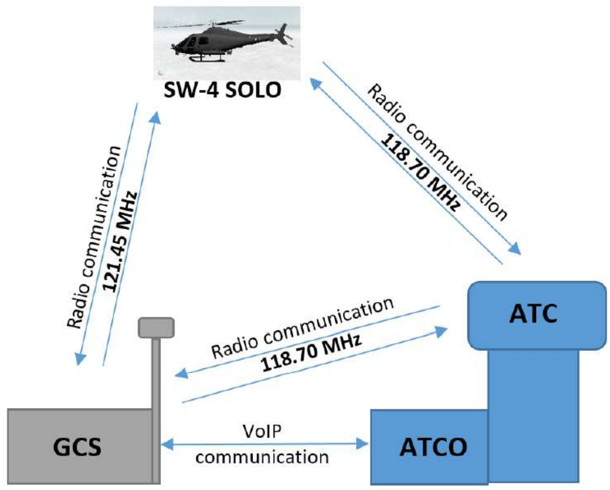

Figure 48: Communication diagram during tests at the Grottaglie airport. Credits: PZL-Świdnik

When flights were conducted in a segregated area R317, that area was managed by ATC Grottaglie and all communication and potential emergencies was provided to ATC Grottaglie.

6. CONCLUSIONS

The paper presents comprehensive analysis of helicopter basic performance and flight mechanics phenomena. These included different tools and modelling techniques and were supplemented with simulation test campaign. As a result, predicted performance and handling qualities met required operational capabilities and safety. This supported PtF issue and allowed proceeding with flight test campaign.

The modification of the PZL SW-4 helicopter made it possible to extend the operational possibilities in particular with operations over sea. A wide range of thesis analysis, both in scale and on a full-size object, made it possible to provide the required evidence confirming the safety of the structure.

From the point of view of utility values, it can be stated that:

- The helicopter equipped with the EFS system has very good buoyancy properties, maintaining stability for sea state conditions 5 min,
- Based on numerical analyzes and laboratory tests of ditching the results allows to determined static strength margin factors for the elements of the floatation system cylinders mounting on the helicopter structure,

- From the point of view of performance, level flight speed and hover deterioration was predicted and confirmed during flight tests, while maintaining required system operational capabilities.
- EFS installation was predicted to have no critical impact on helicopter stability and control margins. This was further confirmed in flight tests.
- Determined the element limiting the static strength of the provision for the floatation system cylinders mounting on the helicopter,
- Determined static strength of the floatation system mounting elements and the landing gear for in-flight cases and normal landings and provided evidence for supporting clearance to an experimental permit to fly acc. to Joint Aviation Regulations JAR 27 (with amendment 27/98/1).
- In the analysis the in-flight loads (mass forces and aerodynamic) and landing loads (related with the speed of contact with ground) of packed and inflated floats were considered and their influence onto the skid and brackets structure.

The part which was concerned on the SATCOM system integration was focused to provide general overview on the aspect to extend the operational possibilities and provide answer on the questions raised by the market – if the helicopter based on the Type Certificate can be the optionally piloted/ unmanned platform with the confirmed capabilities of for the management of an RPAS integrated in ATM operations, in a scenario of both real and simulated traffic.

As more, based on the calculation analyses and as a result of simulation studies together with a ground and flight tests, it can be stated that:

- The installation of satellite communication systems does not affect the safety of the helicopter, without significantly changing its control performance and static and dynamic stability,
- Conducted thermal analyzes and flight tests confirmed the correctness of the SATCOM installation and thus the safety of the structure,
- The data transmission latencies between RPAS and a ground control station caused by the SATCOM datalink and the impact of these delays on air traffic management provide confirmation on the data transfer efficiency and the correctness of the command and control data link system,
- The level of security in the event of a cyber-attack on the Datalink between the helicopter and the ground control station was confirmed as a possible to achieve in the real dangerous aspect conditions.

Author contact:

Adam Rosłowicz adam.roslowicz@leonardo.com

Radosław Raczyński radoslaw.raczynski@leonardo.com

Wiesław Kanadys wieslaw.kanadys@leonardo.com

Jakub Solarski jakub.solarski@leonardo.com

7. ACKNOWLEDGMENTS

HELIMARIS project was conducted as part of the INNOLOT sector project entitled “Modification of an optionally piloted helicopter to maritime mission performance”, coordinated by Wytwórnia Sprzętu Komunikacyjnego “PZL-Świdnik” Spółka Akcyjna, co-financed by the National Centre for Research and Development under the Smart Growth Operational Programme 2014-2020, 1. Priority Axis, Support for R&D activity of Enterprises; Action 1.2, Agreement No. POIR.01.02.00-00.0004/15.

Authors would like to thank HELIMARIS project subcontractors – Warsaw University of Technology and Maritime Advanced Research Centre (CTO S.A.) teams for their support and commitment.

Part of this work was performed within OCEAN 2020 project funded from the European Union's Preparatory Action on Defence Research under grant agreement No 801697.
This presentation reflects only the author's view. The European Defence Agency and the Commission are not responsible for any use that may be made of the information it contains.

8. REFERENCES

1. Łucjanek, W., *Mechanika Lotu. Pomoce do wykładów i ćwiczeń audytoryjnych*, Wydawnictwo Politechniki Warszawskiej, Warszawa, 1978.
2. Topczewski, S., Bibik, P., Narkiewicz, J., „The Final Phase of a Helicopter Automatic Landing on a Vessel’s Deck”, 45th European Rotorcraft Forum Proceedings, Warsaw, September 2019.

3. Kopyt, A., Świętoń, G., "An Objective Assessment Tool (gOAT) of Helicopter Pilot's Performance", 44th European Rotorcraft Forum Proceedings, Delft, September 2018.
4. Tomaszewska, P., Kopyt, A., "A Tool for Pilot's Performance and Engagement Assessment in Helicopter Flight Simulator", 45th European Rotorcraft Forum Proceedings, Warsaw, September 2019.
5. De Silva, C. W., *Modelling of Dynamic Systems*, CRC Press, Boca Raton, 2018.
6. Żugaj, M., Topczewski, S., Bibik, P., Rosłowicz, A., Małecki, J., „The Stability Augmentation System for a Helicopter Landing on a Vessel Deck", 47th European Rotorcraft Forum Proceedings, United Kingdom, September 2021.
7. 45th European Rotorcraft Forum, Warsaw, Poland, 17-20 September, 2019 The use of co-simulation methodology in the project of PZL SW-4 helicopter adaptation to maritime version.
8. https://opennav.com/ - public domain